

# Quantification of collective behaviour via movement tracking

Kirill Lonhus, Dalibor Štys & Renata Rychtáriková

<sup>1</sup>University of South Bohemia in České Budějovice, Faculty of Fisheries and Protection of Waters, South Bohemian Research Center of Aquaculture and Biodiversity of Hydrocenoses, Institute of Complex Systems, Zámek 136, 373 33 Nové Hradky, Czech Republic.

Terms such as *leader*, *follower*, and *oppressed* sound equally well in the description of a pack of wolves, a street protest crowd, or a business team and have very similar meanings. This indicates the presence of some general law or structure that governs collective behaviour. To reveal this, we selected the most common parameter for all levels of the organization – motion. A causality analysis of distance correlations was performed to obtain follow-up networks that show who follows whom and how strongly. These networks characterize an observed system in general and work as an automation bridge between the biological experiment and the broad field of network analysis. The proposed method was tested on a school of aquarium fish. The pattern observed in the network can be easily interpreted and are in agreement with expected behaviour.

## 1 INTRODUCTION

Collective behaviour is one of the most enigmatic phenomena of contemporary times.<sup>1</sup> It is a genuinely omnipresent phenomenon – from flocking of birds and the growth of bacterial colonies<sup>2</sup> to the stock market trading and hierarchy of school classes. We intuitively feel that something should be familiar to all these phenomena because the observed patterns of agents' behaviour, such as *leader*, *follower*, *oppressed*, or *crowd*, sound applicable to all these systems. There is probably some general law or structure common to most living species and unrelated to the level of organization.<sup>3</sup>

This work justifies and formalizes such a general meaning and empirically verify the findings. In order to be able to link such diverse types of collective behaviour, it is necessary to choose its common manifestation. We selected *the motion*. This term has a similar meaning for most groups of living species (a move from "bad" to "good") and is invariant to the organization level (degree of evolution). For instance, cells move from a place without nutrients to a place with nutrients or dogs run away from vehicles.

One of the most common approaches to evaluating motion is the analysis of agents' relative position.<sup>4</sup> This method was successfully applied in the investigation of human behaviour<sup>5</sup> and fish.<sup>6</sup> There are two types of this approach: physically inspired and model-free. The first one assumes a direct analogy with the physical system: agents are considered to be particles driven by potential

– spring-like – forces. These potential-driven particles are the first models that can explain the behaviour of flocks and schools.<sup>3</sup> This set of techniques is an excellent tool for quantifying known phenomena, but not for discovering new ones.

Another – data-driven – approach characterizes the agents’ behaviour by specific, measurable quantities (e.g., the nearest neighbour distance, the Voronoi cell size) and then uses these high-level features to describe observed phenomena. To a certain extent, this approach works, but a more recent paper<sup>7</sup> proved it as insufficient. Therefore, the next generation of models<sup>8</sup> defined a network based on each agent’s position and the sensory field. This step was important towards incorporating the behaviour itself (the individual’s reaction to the observed situation) into the model that would address the decision-making process.

However, this approach is still not fully model free. It assumes that the sensory field is local and attached to the agent, with the interactions themselves being local and homogeneous. Despite the remarkable success, it is hard to extend this approach to include heterogeneous agents and non-local interactions. To address these limitations, we propose a more model-free way to characterizing a group of interacting agents. This approach does not limit interactions by nor type nor locality. Moreover, as we will show in the results, this approach allows the agents to be heterogeneous, which is crucial to explaining the biological experiment results.

We selected a small aquarium fish – Tiger Barb – as a testing subject. This species is very active and keen, able to form shoals from 5 individuals with complex collective behaviour.<sup>9</sup> To track the movement of each fish without any label, we employed video analysis.

## 2 RESULTS

### Fish tracking

During the experiment, the aquarium with fish was recorded with a frequency of 25 Hz. The images were stored uncompressed in the 16-bit depth. Before further processing, we had to separate the camera images into corresponding views. The aquarium corners were annotated manually (total 28 points) and then fitted by a projective transformation. As a side effect, the projective transformation compensated for the distortion of the corresponding views (Figure 1) and the aspect ratio became linearly proportional to the actual size of the aquarium.

The aquarium front view giving the  $z$ -coordinates of the fish localization was always processed separately. The bottom and top views were almost the same but only mutually flipped (in terms of coordinates  $x, y$ ) and, thus, were usually averaged. In case that the fish were overlapping in the top view and not in the bottom view (or vice versa), the bottom and the top view were processed separately to give better tracks. The general method pipeline (Figure 2A) was inspired

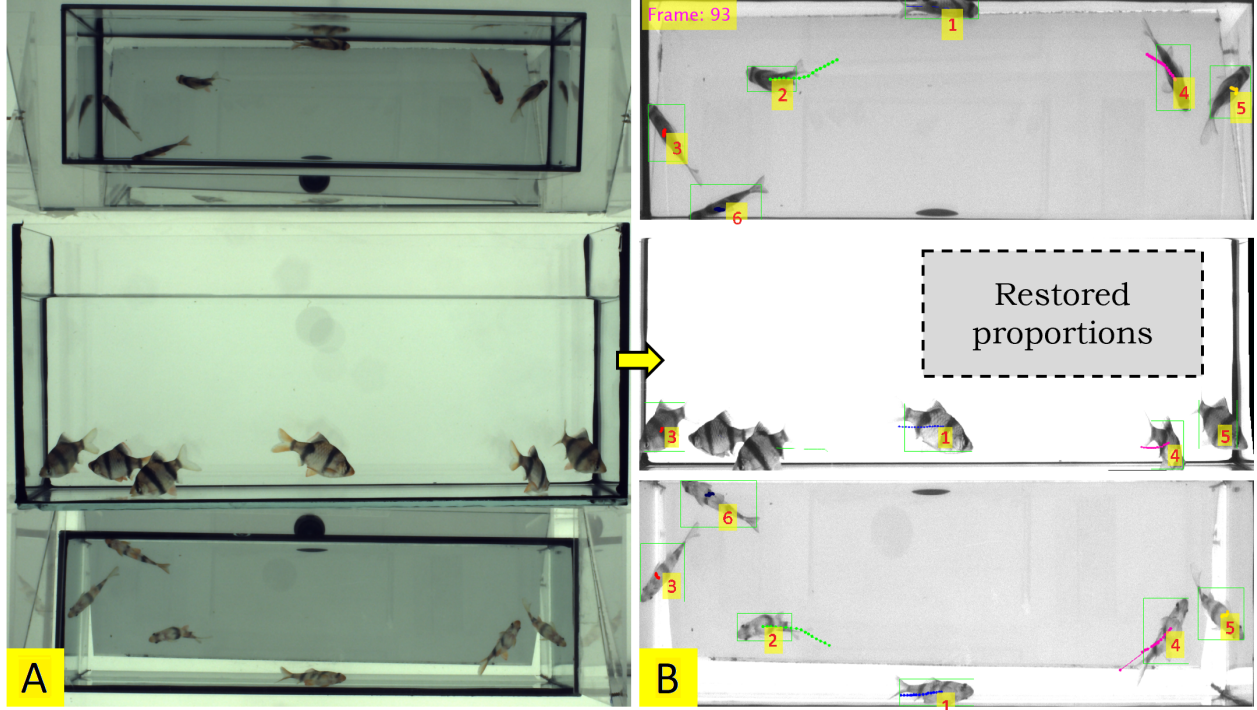


Figure 1: **(A)** The experimental setup (a fish aquarium with two side mirrors) and **(B)** individual objects (fish) tracking in the multiple views after image geometry restoration.

by Perez-Escudero et al.<sup>10</sup> and Romero-Ferrero et al.<sup>6</sup> but rewritten from scratch. The original algorithm is 2D, but, in our case, three 2D views allow us the reconstruction of 3D positions (with  $x-y$  redundancy when one view is from above and the second one is from below the aquarium) using re-projecting the coordinates and calculating the overlap of coordinates between the assembled trajectories in different views. This allows us to permute the classifiers that were the first (for all views) to detect the same fish in the corresponding views. In this way, we get a consistent annotation between views.

In the first step, a simple foreground detection, based on median background estimation, was used. This foreground detection is very robust and showed a high recall. The detected objects were then classified as individuals/overlaps using a small VGG-like CNN.<sup>11</sup> This CNN annotation was generated automatically, based on average areas and perimeters of the detected objects. The detections for each fish were assembled into contiguous sequences – tracklets – based on the overlapping their bounding boxes in every two consecutive frames. In some cases, it was possible to resolve the overlaps of two fish<sup>12</sup> to increase the continuity of the tracklets.

The image sequences, where the number of detected objects coincides with the number of the fish in the experiment, were used as seeds for the next CNN-based classifier. These sequences for the different aquarium sides were matched using projection of coordinates and overlap in the time

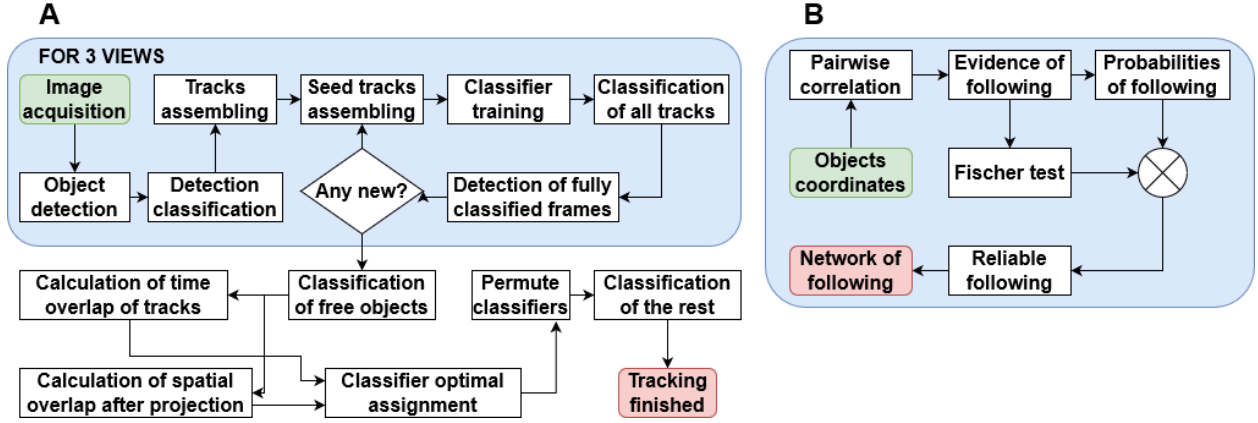


Figure 2: **(A)** The extraction of objects' coordinates and tracking algorithm. **(B)** The algorithm for construction of follow-up networks. This algorithm arises from the tracking algorithm **A**.

domain<sup>10</sup> and used for training the classifier. Then, all objects were classified. Among them, the trustworthy sequences were selected and used for training. Four passes were typically enough to achieve a high (0.98) classification accuracy. In the same way, the whole tracklets were classified. The tracklets from different views were projected (using known proportion between coordinates) and merged, giving 3D coordinates [mm].

Specific post-processing steps were applied to fill the gaps in the trajectories (where it was possible to do it unambiguously via overlap uniqueness) by a simple linear interpolation between the ends of the parts of the trajectories. We verified the method accuracy only visually. However, the method was designed similarly to Perez-Escudero et al.<sup>10</sup> and, thus, its accuracy is assumed to be comparable. Due to the design of the method, visual inspection of the fish trajectories has not shown any significant errors. The output of this step is a time-resolved 3D trajectory of each fish. We intentionally did not describe the tracking algorithm in-depth because the processing and analysis below are not narrowly limited to this data but also suitable to any position tracking data. The complete code with comments is available in supplementary materials.

## Determination of temporal correlations

To compare the results for different species/levels of organization, we needed to decouple the behaviour from the motion. For this, the distance correlation was used. The idea was simple – to rewrite the classical covariance by the multiplication of the signed distances. Let  $A, B$  be scalar sequences of length  $N$ , then

$$\text{cov}(A, B) = \frac{1}{N^2} \sum_i^N \sum_j^N (A_i - A_j) \cdot (B_i - B_j) = \frac{1}{N^2} \sum_i^N \sum_j^N D_{ij}(A) \cdot D_{ij}(B) \quad (1)$$

where  $D_{ij}(X)$  is a signed distance between elements  $i$  and  $j$  of arbitrary sequence  $X$ . If we replace such a signed distance by the Euclidean distance  $D_{ij}(\vec{X}) = \|\vec{X}_i - \vec{X}_j\|$ , the obtained function will behave very similar to the classical covariance and let us denote it as a distance covariance. Such a definition allows us to introduce a Pearson-like correlation coefficient, which we denoted the distance correlation, by replacing the covariances with the distance covariances:

$$\text{corr}(\vec{A}, \vec{B}) = \mathbf{N}^2 \frac{\sum_{i,j} \|\vec{A}_i - \vec{A}_j\| \cdot \|\vec{B}_i - \vec{B}_j\|}{(\sum_{i,j} \|\vec{A}_i - \vec{A}_j\|^2) \cdot (\sum_{i,j} \|\vec{B}_i - \vec{B}_j\|^2)}, \quad (2)$$

where  $\vec{A}, \vec{B}$  are vector sequences with the length of  $\mathbf{N} = \{\dots, i, j, \dots\}$  points in the Euclidean space of the same dimensionality. Despite its simplicity, this method was rigorously done and investigated quite recently.<sup>13</sup> However, it varies from  $[0, 1]$  instead of  $[-1, 1]$ , which is a direct consequence of the presence of the unsigned distance. As shown in even more recent paper,<sup>14</sup> such characteristics shows most of the properties and common meaning of the ordinary correlation.

We used the correlation in Equation (2) as a measure of the trajectories' similarity in the most general sense. The correlation between positions in a sliding window for two selected objects on a timeline gave the local similarity of their motion (Figure 3A).

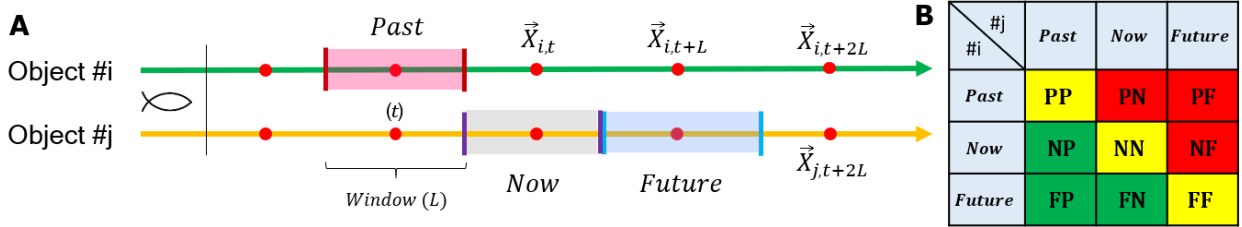


Figure 3: (A) The timelines for two objects with relevant correlation time windows of the length  $L$ . (B) The favourable (**green**), neutral (**yellow**), and unfavourable (**red**) combinations of correlations for a situation when object  $i$  follows object  $j$ . Symbols **P**, **N**, and **F** denotes the past, current, and future states of the object  $i$  or  $j$ , respectively.

It is also possible to select windows mutually shifted on the time arrow. For an object, let us select three dedicated time windows centred at times  $t$ ,  $t - L$ , and  $t + L$ , respectively, where  $L$  is a window size, and denote them as **Past**, **Now**, and **Future**. Thus, any pair of objects gives 9 combinations for two windows. Let us denote the time windows by two-letter codes: the first letter marks the first object's time state, the second letter is for the second object's time state. For example, **PF** means a comparison of the first object's past position with the second object's future position. This notation helped us to analyse the physical interpretation and causality of such shifted correlations.

## Construction of follow-up networks

Let us define the term *following* in this way: if object  $i$ 's *future state* correlates with object  $j$ 's *past state*, then *object  $i$  follows object  $j$* .

If we consider the hypothesis that  $i$  follows  $j$  then combinations of time windows can be classified into 3 groups (Figure 3B): supporting the hypothesis  $S = \{\mathbf{NP}, \mathbf{FP}, \mathbf{FN}\}$ , neutral to the hypothesis  $N = \{\mathbf{PP}, \mathbf{NN}, \mathbf{FF}\}$ , and rejecting the hypothesis  $R = \{\mathbf{PN}, \mathbf{PF}, \mathbf{NF}\}$ . If each time window is taken from each group always only once, it gives  $3^3$  combinations. We denoted as an evidence the fact that one correlation is higher than another. Such an evidence is treated as significant if the corresponding correlation is higher than the correlation from the neutral group. In the next step, we evaluated the statistical significance of the hypothesis whether the tendency that object  $i$  follows object  $j$  and vice versa is higher than that object  $j$  follows object  $i$ . For each pair of objects  $i$  and  $j$ , we have four possibilities how the objects follow each other in a time window:  $i$  follows  $j$ ,  $j$  follows  $i$ ,  $i$  does not follow  $j$ ,  $j$  does not follow  $i$ . The algorithm for the construction of follow-up networks is depicted in Figure 2B.

The total numbers of the significant evidences during the experiment are

$$e^{(i \rightarrow j)} = \sum_{s^{(i \rightarrow j)}}^{S^{(i \rightarrow j)}} \sum_n^N \sum_{r^{(i \rightarrow j)}}^{R^{(i \rightarrow j)}} [s^{(i \rightarrow j)} > n] \cdot [s^{(i \rightarrow j)} > r^{(i \rightarrow j)}], \quad (3)$$

$$e^{(j \rightarrow i)} = \sum_{s^{(j \rightarrow i)}}^{S^{(j \rightarrow i)}} \sum_n^N \sum_{r^{(j \rightarrow i)}}^{R^{(j \rightarrow i)}} [s^{(j \rightarrow i)} > n] \cdot [s^{(j \rightarrow i)} > r^{(j \rightarrow i)}], \quad (4)$$

$$e^{(i \nrightarrow j)} = \sum_{r^{(i \nrightarrow j)}}^{R^{(i \nrightarrow j)}} \sum_n^N \sum_{s^{(i \nrightarrow j)}}^{S^{(i \nrightarrow j)}} [r^{(i \nrightarrow j)} > n] \cdot [r^{(i \nrightarrow j)} > s^{(i \nrightarrow j)}], \quad (5)$$

$$e^{(j \nrightarrow i)} = \sum_{r^{(j \nrightarrow i)}}^{R^{(j \nrightarrow i)}} \sum_n^N \sum_{s^{(j \nrightarrow i)}}^{S^{(j \nrightarrow i)}} [r^{(j \nrightarrow i)} > n] \cdot [r^{(j \nrightarrow i)} > s^{(j \nrightarrow i)}], \quad (6)$$

where  $e^{(i \rightarrow j)}$ ,  $e^{(j \rightarrow i)}$ ,  $e^{(i \nrightarrow j)}$ , and  $e^{(j \nrightarrow i)}$  are sums of significant evidences when object  $i$  follows object  $j$ , object  $j$  follows object  $i$ , object  $i$  does not follow object  $j$ , and object  $j$  does not follow object  $i$ , respectively. Variables  $s^{(i \rightarrow j)}$  and  $s^{(j \rightarrow i)}$  denote correlations supporting the hypothesis that object  $i$  follows object  $j$  and vice versa, respectively. The analogous variables  $r^{(i \rightarrow j)}$  and  $r^{(j \rightarrow i)}$  denote correlations rejecting the hypothesis that object  $i$  follows object  $j$  and vice versa,

respectively. Variable  $n \in N$  is a combination of time windows that is neutral to the hypothesis of following up.

The discrete sums of the significant evidences in Equations (3)–(6) were first used as an input into the Fisher exact test<sup>15</sup> to calculate the precise  $p$ -value. In this case, the meaning of the  $p$ -value is a measure of the deviation from the hypothesis that no one follows anyone. From Table 1 the  $p$ -value of the Fisher test was calculated as

$$\begin{aligned}
 p &= \frac{\binom{e^{(i \rightarrow j)} + e^{(j \rightarrow i)}}{e^{(i \rightarrow j)}} \binom{e^{(i \nrightarrow j)} + e^{(j \nrightarrow i)}}{e^{(i \nrightarrow j)}}}{\binom{e^{(i \rightarrow j)} + e^{(j \rightarrow i)} + e^{(i \nrightarrow j)} + e^{(j \nrightarrow i)}}{e^{(i \rightarrow j)} + e^{(j \rightarrow i)}}} \equiv \frac{\binom{e^{(i \rightarrow j)} + e^{(j \rightarrow i)}}{e^{(j \rightarrow i)}} \binom{e^{(i \nrightarrow j)} + e^{(j \nrightarrow i)}}{e^{(j \nrightarrow i)}}}{\binom{e^{(i \rightarrow j)} + e^{(j \rightarrow i)} + e^{(i \nrightarrow j)} + e^{(j \nrightarrow i)}}{e^{(j \rightarrow i)} + e^{(j \nrightarrow i)}}} \equiv \\
 &\equiv \frac{(e^{(i \rightarrow j)} + e^{(j \rightarrow i)})! (e^{(i \nrightarrow j)} + e^{(j \nrightarrow i)})! (e^{(i \rightarrow j)} + e^{(i \nrightarrow j)})! (e^{(j \rightarrow i)} + e^{(j \nrightarrow i)})!}{e^{(i \rightarrow j)}! e^{(j \rightarrow i)}! e^{(i \nrightarrow j)}! e^{(j \nrightarrow i)}! (e^{(i \rightarrow j)} + e^{(j \rightarrow i)} + e^{(i \nrightarrow j)} + e^{(j \nrightarrow i)})!}.
 \end{aligned} \tag{7}$$

The relations  $i$ - $j$ , i.e., the time windows, whose  $p$ -values lie under the criterion of level of significance  $\alpha = 0.05$  (i.e.,  $p \leq C_\alpha$ ) were rejected. This removing of spurious correlations<sup>16</sup> greatly improved the robustness of the obtained networks.

For the rest of relations  $i$ - $j$ , the *follow-up probabilities* were then defined using the sums of significant evidences written in Eqs. 3–6, e.g.,

$$P^{(i \rightarrow j)} = \frac{e^{(i \rightarrow j)}}{e^{(i \rightarrow j)} + e^{(i \nrightarrow j)}} = [1 + \frac{e^{(i \nrightarrow j)}}{e^{(i \rightarrow j)}}]^{-1}, \tag{8}$$

where  $P^{(i \rightarrow j)}$  is a chance that object  $i$  follows object  $j$ . The advantage of the proposed measure of following up is not only its clear meaning but also the fact that it decoupled from direct measurements: first its transformation to correlation space, and then from correlation space to probability space. Thus, it allows us the comparison and general analysis of very different systems, because even absolute values of correlation are not matters, only their combinations and ratios. The obtained following matrix is of the size  $n_{obj} \times n_{obj}$  in case of  $n_{obj}$  objects and is typically sparse, thus it is natural to convert it to a directed graph (treating the following matrix as an adjacency matrix). The orientation of the network edges follows the comparison of the values of probabilities  $P^{(i \rightarrow j)}$  and  $P^{(j \rightarrow i)}$ . Examples of such graphs (visualized in a way that a higher follow-up probability corresponds to a shorter edge) are shown in Figure 4A. These graphs are defined at each recorded time (Video in Supporting files) and have a very clear behaviouristic meaning, showing who follows whom.

The approach described above utilizes only a single parameter – the size of the time window  $L$ . The obtained network is thus a function only of the time  $t$  and the parameter  $L$ .

## Biological relevance

In order to verify the method, we conducted a straightforward experiment: the fish were freely swimming in an aquarium for 15 min. The experiment was repeated ten times on different days to investigate the stability of the fish school and the repeatability of measurements. An output of the method is a directed graph defined for each time frame (Video in Supporting files). Interpretation of these graphs is straightforward: the nodes correspond to the observed objects (fish individuals in our case), length of the edges inversely reflect the follow-up probability (the shorter the edge, the higher the chance of following up). The arrows show who follows whom.

In order to show the variability of the follow-up network over time, we partition the graphs adjacency matrices into two groups by  $k$ -means. Figure 4A shows the follow-up networks dominating in each of the groups. Of course, the real situation is more complicated, and two groups of the follow-up networks are only the minimal illustrative example. The networks (Figure 4A) are almost the same, but directions of edges are opposite and fish #1 and #6 swapped their positions. Fish #3 situated in the centre has the most prominent set of features among all. Even without biological analysis, one can assess that this fish is somehow important. Fish #3 has relatively strong connectivity to all other fish and is completely changing its role in the school (depicted by a reverse direction of the network edges). Fish #2 is also connected to everyone, but the connections are weak (the lengths of network edges are relatively long). Fish #5 and #6 changed their mutual distances in the graphs and did not show distinct features.

The number of edges entering/emerging from a network node in a time window characterizes the in/out-degree. For each node, two centrality measures – in-degree and out-degree – quantifies the intensity of the relations among the fish. After that, for all ten experiments, a probability density function for values of in/out-degree parameters was estimated by the kernel density estimation (Figure 4B). The obtained distribution is nor unimodal nor trivial. In order to switch to the parametric statistics, a mixture of 4 Gaussians was fitted to this distribution (Figure 4B). Then, both in- and out-degree parameters can be described by four sets of [component proportion, mean value, variance] corresponding to one peak in the distribution.

The component (peak area) proportions in the probability density functions (compared with mean values or variances) provides the clearest interpretation of the results – this approach is closely related to frequency analysis. A higher value of the component proportion corresponds to a longer time spent in the relevant mean value (the components are sorted in ascending order according to the mean values). A robust measure of in/out-degree due to a relatively low frequency of occurrence is a sum of the 3<sup>rd</sup> and the 4<sup>th</sup> component proportion, showing how frequently the fish exhibits a high in/out-degree state. The box plot of in-degree states for all six fish from 10 experiments is depicted in Figure 4C. Fish #3 and #4 show the highest in-degree state. These individuals are frequently followed and literally *lead* the school. However, #3 has a low out-degree and rarely follows someone, whereas #4 has a high out-degree. We interpret this as meaning that



fish #3 is a leader, whereas fish #4 can be called a coordinator. As supported in Figure 4A, the issue is that there is no clear definition of possible roles, only a consensus that they exist.<sup>17</sup> The role of the *coordinator* changes diametrically (the coordinator can be followed or following). In general, such a network shows an oscillatory process over time and is not trivial (it is impossible to obtain from one cluster another by simply changing the direction of edges). We have not investigated this phenomenon deeper yet, but a similar oscillation process has been already observed before.<sup>18</sup> The mean value, which corresponds to the out-degree Gaussian components 3 and 4 for fish #1, is significantly lower than the average (Figure 4D). The combination with a very low in-degree component proportion may support the hypothesis that fish #1 is *oppressed* or, more precisely, *unsocial*. Fish #1 is never a leader but also does not follow the school too much.

Thus, even this most simple analysis of the obtained graphs gives an insight into the school structure, which is consistent between the experiments. Of course, the detected *roles* have to be rigorously tested in different schools, even with different species. Nevertheless, the complexity of the observed phenomena is quantifiable. Our results are in agreement with the trend recently published in research papers<sup>17,19,20</sup> that variability in individual behaviour matters in collective behaviour. We think that this variability is essential to explain the observed phenomena. Despite this, further studies will be needed, including a detailed comparison of the obtained results with visual observations.

### 3 DISCUSSION AND CONCLUSIONS

The approach to collective movement quantification proposed in this paper is both informative and easy to interpret. It can be applied to any kind of multiple trajectory data, irrelevant to the species, level or even type of organization (e.g., for flocks of drones or military ships). The approach has only one adjustable parameter – the time window selected according to the system type – making the method effectively model-free, giving a spectrum of networks for all windows.

Even a limited application such as a single group of a single species showed a fascinating result: the observed roles in the school are not demonstrated all the time, but rather for a time of necessity. This fact addresses a pitfall of many psychological approaches, which assign a single personality type (temperament or MBTI model<sup>21</sup>) to an agent unambiguously and then predict interactions based on this assignment. However, it does not work in this way, and we can see why: even very primitive species show flexible roles dependent on a given situation. It is more suitable to speak about the distribution of such assignments (attributes, categories) or, better, conditional distributions of the roles.

The obtained results also point to pitfalls of classical – homogeneous – agent models: even in our simple experiments, the agents received a set of parameters that differed significantly from each other and could be named as *personality* with considerable caution. We believe that individual variability is essential to the observed collective phenomena, but we should conduct additional

experiments to prove this.

The main advantage of the proposed method, however, is not its generality but its applicability. The method allows to convert widespread, well-known tracking data to the time-dependent directed graphs (sometimes called coevolution networks<sup>22,23</sup>), which are one of the hottest topics of modern data mining<sup>24</sup> and collective behaviour analysis.<sup>25</sup>

We expect this method to benefit all parties – biologists and data scientists – and encourage further collaboration and knowledge transfer.

### **Code availability**

The Matlab code is available at Dryad.<sup>26</sup>

### **Supporting files**

**Video.**<sup>26</sup> Time changes of the follow-up networks (i.e., fish school configurations) during the experiment. Top view (*upper left*), bottom view (*upper right*), front view (*lower left*) of fish school in the aquarium, and follow-up network (*lower right*).

### **Author contributions statement**

KL collected the image data; he is the developer of the algorithm and the main author of the paper. RR proofread the paper and contributed critically to the results. DŠ is the group leader responsible for funding the research and the inventor of the aquarium device.

### **Competing interests**

All authors declare no conflict of interests.

### **Funding**

This work was supported by the Ministry of Education, Youth and Sports of the Czech Republic—projects CENAKVA (LM2018099) and from the European Regional Development Fund in frame of the project ImageHeadstart (ATCZ215) in the Interreg V-A Austria–Czech Republic programme. The work was further financed by the project GAJU 017/2016/Z.

## 4 METHODS AND MATERIALS

### Fish breeding

As a model organism, we used a Tiger Barb (*Puntigrus tetrazona*) in a group of 6 individuals.

Between the experiments, the fish lived in a relatively large home aquarium ( $60 \times 35 \times 40$  cm<sup>3</sup>). The aquarium was disinfected with ethanol, boiling, and sodium hydrogen carbonate and designed to simulate the natural environment with involved aquatic plants and stones (4–8 mm). The fish were bred at a 12/12 artificial daylight cycle and 25 °C. The water quality was validated at weekly intervals and before each experiment. The parameters of water were temporarily adjusted according to the conditions prevailing in the aquarium:  $4.9 \text{ g} \cdot \text{L}^{-1} \text{ Mg}^{2+}$ ,  $12.0 \text{ g} \cdot \text{L}^{-1} \text{ Ca}^{2+}$ ,  $5.5 \text{ g} \cdot \text{L}^{-1} \text{ NO}_3^-$ , pH 6.9, hardness 2.8 °H. The aquarium was equipped with a Sera LED 360, a Sera Air 110 air pump, a Sera Fil Bioactive 130 L separate filter (all from Heinsberg, Germany), and a water heater. The fish were fed (predominantly by the Tetra Min, Tetra, Melle, Germany) once a day (at 7 a.m.), always 1 h after turning on the aquarium illumination.

### Image data collection

The experiments were conducted at  $(11 \pm 0.5)$  a.m. on 10 consecutive days (including the weekend). The condition of the fish was assessed before each experiment. Figure 1 represents the experimental set-up. The small ( $38.5 \times 20 \times 14$  cm<sup>3</sup>, maximal volume 8-L; 6-L used) aquarium was located inside a LED box, which provided homogeneous illumination from all angles. Water in the aquarium came from the home aquarium. Along four sides of the aquarium, mirrors were located. Two – above and below the aquarium – mirrors were sufficient to observe the aquarium from 3 sides simultaneously (one side directly and two sides in mirrors). The fish were transported to the small aquarium under full illumination 5 min before each experiment. Of course, such a setup may cause significant stress to the fish. However, the previous exposure of the fish to light significantly mitigated the behaviour alteration. In addition, this species has a keen intellect and good memory, so the experimental conditions are not new for it every day, and the stress is alleviated. Above all, the aim was not to fully eliminate the stress but to make it repeatable and systematic so that all fish perceive the stress equally. All experiments were performed with a single group of fish in order to eliminate inter-group variability. It is unknown how different school structures can be (even for the same species and group size).

In order to reduce the number of errors in identifying individual fish, the data was collected by a 12-bit Ximea MX124CG-SU-X2G2-FAB rgb camera (scanning frequency 0.4 Hz). The size of the fish in the digital image corresponded to approx.  $50 \times 30$  px ( $5 \mu\text{m}^2 \cdot \text{px}^{-1}$ ).

## ABBREVIATIONS AND SYMBOLS

$A_i, A_j$	position (scalar) of the first object in two consecutive time windows $i$ and $j$ , respectively (in our specific case $A \equiv X_i$ )
$B_i, B_j$	position (scalar) of the second object in two consecutive time windows $i$ and $j$ , respectively (in our specific case $B \equiv X_j$ )
$\vec{A}_i, \vec{A}_j$	vector position of the first agent in frames $i$ and $j$ , respectively (in our specific case $\vec{A} \equiv \vec{X}_i$ ); $\vec{A}_i = (x_{Ai}, y_{Ai}, z_{Ai})$ and $\vec{A}_j = (x_{Aj}, y_{Aj}, z_{Aj})$ in the 3D Euclidian space
$\vec{B}_i, \vec{B}_j$	vector position of the second agent in frames $i$ and $j$ , respectively (in our specific case $\vec{B} \equiv \vec{X}_j$ ); $\vec{B}_i = (x_{Bi}, y_{Bi}, z_{Bi})$ and $\vec{B}_j = (x_{Bj}, y_{Bj}, z_{Bj})$ in the 3D Euclidian space
$C_\alpha$	$\alpha$ -dependent criterion of the Fisher test
CNN	convolutional neural network
$D_{ij}$	difference between the scalar distances in two consecutive time frames $i$ and $j$
$e$	frequency of occurrence of significant evidences in the experiment
<b>F</b>	agent's future state (location)
<b>FF</b>	follower's and leader's future states correlate (neutral hypothesis)
<b>FN</b>	follower's future state correlates with leader's current state (supporting hypothesis)
<b>FP</b>	follower's future state correlates with leader's past state (supporting hypothesis)
$i, j$	labels of agents (fish)
$i, j$	labels of two consecutive time windows in the image sequences; $i, j \in \mathbb{N}$
$i \rightarrow j$	agent $i$ follows agent $j$
$i \not\rightarrow j$	agent $i$ does not follow agent $j$
$j \rightarrow i$	agent $j$ follows agent $i$
$j \not\rightarrow i$	agent $j$ does not follow agent $i$
$k$	number of clusters in $k$ -means analysis
KDE	kernel density function
$L$	size of the time window
$n$	element of the set $N$
$n_{obj}$	number of agents in the experiment; $n_{obj} = 6$ fish
$N$	set of combinations of time windows having no relation to the hypothesis that one object follows another one; $N = \{\mathbf{PP}, \mathbf{NN}, \mathbf{FF}\}$
<b>N</b>	number of time windows in the sequences
<b>N</b>	agent's current state (location)
<b>NF</b>	follower's current state correlates with leader's future state (rejecting hypothesis)
<b>NN</b>	follower's and leader's current states correlate (neutral hypothesis)
<b>NP</b>	follower's current state correlates with leader's past state (supporting hypothesis)
$p$	$p$ -criterion of the Fisher exact test
$P$	follow-up probability that one agent follows another
<b>P</b>	agent's past state (location)
<b>PF</b>	follower's past state correlates with leader's future state (rejecting hypothesis)
<b>PN</b>	follower's past state correlates with leader's current state (rejecting hypothesis)
<b>PP</b>	follower's and leader's past states correlate (neutral hypothesis)

$r$	element of the set $R$
$R$	set of combinations of time windows rejecting the hypothesis that one object follows another one; $R = \{\mathbf{PN}, \mathbf{PF}, \mathbf{NF}\}$
$s$	element of the set $S$
$S$	set of combinations of time windows supporting the hypothesis that one object follows another one; $S = \{\mathbf{NP}, \mathbf{FP}, \mathbf{FN}\}$
$t$	time; the center of the time window
VGG	Visual Geometry Group (at the Oxford University)
$\alpha$	level of statistical significance

## REFERENCES

1. Bak-Coleman, J. B. *et al.* Stewardship of global collective behavior. *Proceedings of the National Academy of Sciences* **118**, e2025764118 (2021).
2. Gibbs, K. A., Urbanowski, M. L. & Greenberg, E. P. Genetic determinants of self identity and social recognition in bacteria. *Science* **321**, 256–259 (2008).
3. Vicsek, T. & Zafeiris, A. Collective motion. *Physics Reports* **517**, 71–140 (2012).
4. Brown, A. E. X. & de Bivort, B. Ethology as a physical science. *Nature Physics* **14**, 653–657 (2018).
5. Warren, W. H. Collective motion in human crowds. *Current Directions in Psychological Science* **27**, 232–240 (2018).
6. Romero-Ferrero, F., Bergomi, M. G., Hinz, R. C., Heras, F. J. H. & de Polavieja, G. G. id-tracker.ai: tracking all individuals in small or large collectives of unmarked animals. *Nature Methods* **16**, 179–182 (2019).
7. Strandburg-Peshkin, A. *et al.* Visual sensory networks and effective information transfer in animal groups. *Current Biology* **23**, R709–R711 (2013).
8. Davidson, J. D. *et al.* Collective detection based on visual information in animal groups. *Journal of The Royal Society Interface* **18**, 20210142 (2021).
9. de Vries, H. An improved test of linearity in dominance hierarchies containing unknown or tied relationships. *Animal Behaviour* **50**, 1375–1389 (1995).
10. Perez-Escudero, A., Vicente-Page, J., Hinz, R. C., Arganda, S. & de Polavieja, G. G. id-Tracker: tracking individuals in a group by automatic identification of unmarked animals. *Nature Methods* **11**, 743–748 (2014).
11. Liu, S. & Deng, W. Very deep convolutional neural network based image classification using small training sample size. In *2015 3rd IAPR Asian Conference on Pattern Recognition (ACPR)*, 730–734 (IEEE, 2015).

12. Lonhus, K., Štys, D., Saberioon, M. & Rychtáriková, R. Segmentation of laterally symmetric overlapping objects: application to images of collective animal behavior. *Symmetry* **11**, 866 (2019).
13. Székely, G. J., Rizzo, M. L. & Bakirov, N. K. Measuring and testing dependence by correlation of distances. *The Annals of Statistics* **35**, 2769–2794 (2007).
14. Székely, G. J. & Rizzo, M. L. Brownian distance covariance. *The Annals of Applied Statistics* **3**, 1236–1265 (2009).
15. Fisher, R. A. On the interpretation of  $X^2$  from contingency tables, and the calculation of P. *Journal of the Royal Statistical Society* **85**, 87 (1922).
16. Farine, D. R. A guide to null models for animal social network analysis. *Methods in Ecology and Evolution* **8**, 1309–1320 (2017).
17. Marras, S. & Domenici, P. Schooling fish under attack are not all equal: some lead, others follow. *PLoS ONE* **8**, e65784 (2013).
18. Swain, D. T., Couzin, I. D. & Leonard, N. E. Coordinated speed oscillations in schooling killifish enrich social communication. *Journal of Nonlinear Science* **25**, 1077–1109 (2015).
19. del Mar Delgado, M. *et al.* The importance of individual variation in the dynamics of animal collective movements. *Philosophical Transactions of the Royal Society B: Biological Sciences* **373**, 20170008 (2018).
20. Shaw, A. K. Causes and consequences of individual variation in animal movement. *Movement Ecology* **8**, 12 (2020).
21. Briggs-Myers, I. & Briggs-Myers, P. *Gifts Differing* (John Murray Press, 1995).
22. Farajtabar, M. *et al.* COEVOLVE : a joint point process model for information diffusion and network evolution. *Journal of Machine Learning Research* **18**, 49 (2017).
23. Wang, W., Liu, Q.-H., Liang, J., Hu, Y. & Zhou, T. Coevolution spreading in complex networks. *Physics Reports* **820**, 1–51 (2019).
24. Liu, X. F., Chen, H.-J. & Sun, W.-J. Adaptive topological coevolution of interdependent networks: Scientific collaboration-citation networks as an example. *Physica A: Statistical Mechanics and its Applications* **564**, 125518 (2021).
25. Davidson, J. D., Vishwakarma, M. & Smith, M. L. Hierarchical approach for comparing collective behavior across scales: cellular systems to honey bee colonies. *Frontiers in Ecology and Evolution* **9**, 581222 (2021).
26. Lonhus, K., Štys, D. & Rychtáriková. Quantification of collective behaviour via movement tracking – Supplementaries. *Dryad, Dataset* (2021).

Table 1: The Fisher test contingency table for verification of the hypothesis of measure of following up.

	Object $i$	Object $j$	Total rows
Following	$e^{(i \rightarrow j)}$	$e^{(j \rightarrow i)}$	$e^{(i \rightarrow j)} + e^{(j \rightarrow i)}$
Not following	$e^{(i \nrightarrow j)}$	$e^{(j \nrightarrow i)}$	$e^{(i \nrightarrow j)} + e^{(j \nrightarrow i)}$
Total columns	$e^{(i \rightarrow j)} + e^{(i \nrightarrow j)}$	$e^{(j \rightarrow i)} + e^{(j \nrightarrow i)}$	$e^{(i \rightarrow j)} + e^{(i \nrightarrow j)} + e^{(j \rightarrow i)} + e^{(j \nrightarrow i)}$

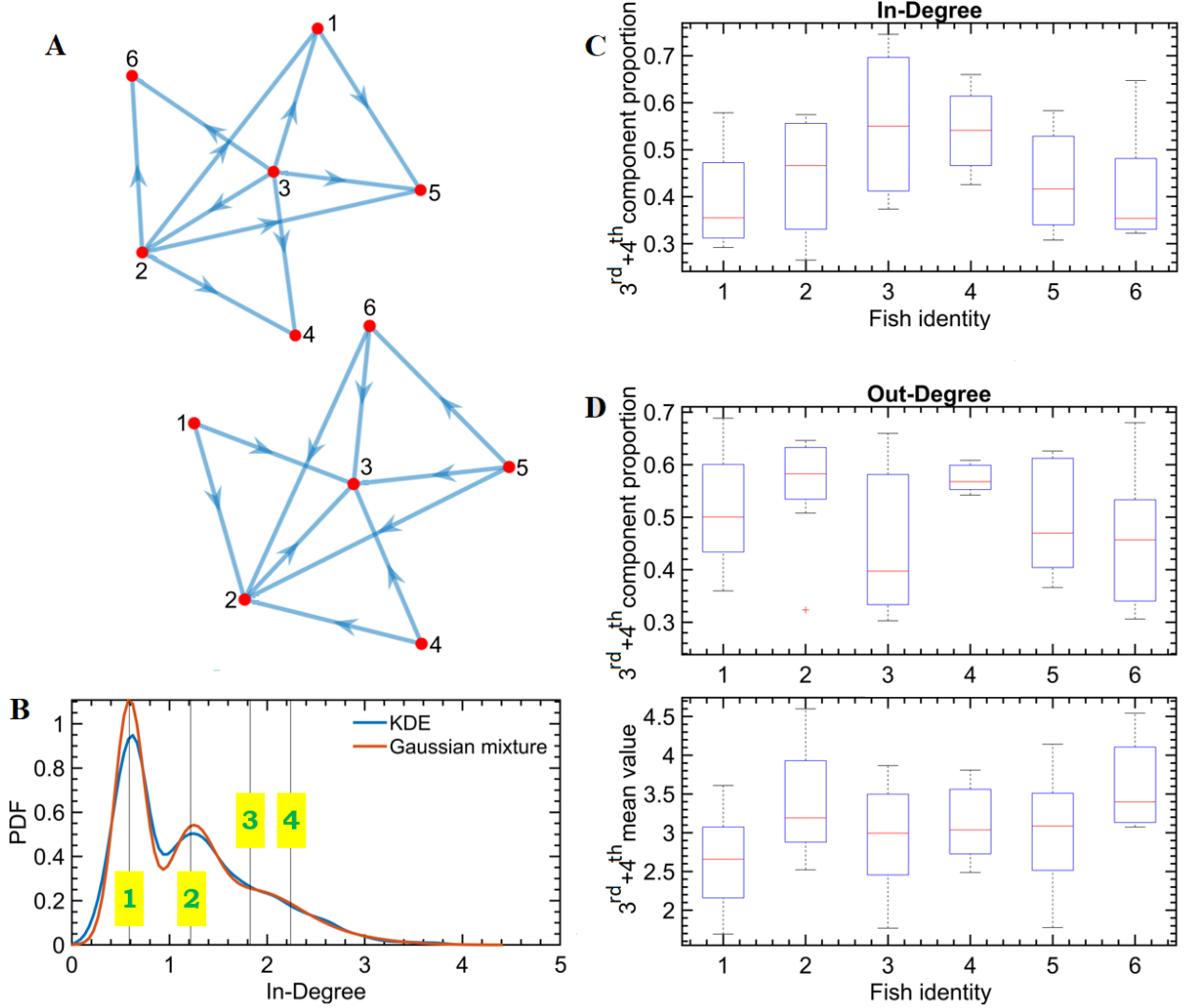


Figure 4: (A) Two typical follow-up networks in a school of 6 fish. (B) The kernel density estimation (KDE) and the Gaussian fitting for the in-degree parameter of the follow-up network. For out-degree parameter, the distributions are analogous to the in-degree parameter. (C) The distribution of intra-experiment in-degree Gaussian fitting component proportions. (D) The distribution of intra-experiment out-degree Gaussian fitting component proportions and mean values.